Impact of the underside velocity on the drag reduction of a trailer model using a passive control system

M. Szmigiel, T. Castelain, M. Michard, D. Chacaton, D. Juvé

Impact of the underside velocity on the drag reduction of a trailer model using a passive control system

M. Szmigiel[1,2], T. Castelain[2], M. Michard[2], D. Chacaton[1] and D. Juvé[2]

1 - Volvo Group Truck Technology, Renault Trucks SAS, Cab Engineering Lyon, 99 route de Lyon, 69806 Saint-Priest Cedex

2 - LMFA UMR CNRS 5509, Ecole Centrale de Lyon, 36 Avenue Guy-de-Collongue, 69134 Ecully Cedex

Abstract: The effect of passive control (inclined boat-tails) on the flow in the wake of a 1:43 scale simplified trailer model is experimentally studied for various underside flow conditions. Base pressure measurements show that the boat-tails allows increasing the base pressure whatever are underside flow velocities studied and the base pressure distribution is always symmetric in the vertical mid plane. In addition, according to the underside flow velocity, the near-wake flow structure consists of a recirculating area attached or completely detached from the ground.

Keywords: Heavy duty, passive control, drag reduction, underbody velocity, experiments

1. Problem statement and experimental set-up

In the road haulage industry, one of main issues is to reduce the fuel consumption. This can be achieved by improving engine performance, reducing the tire rolling resistance but also the aerodynamic drag. The geometry and the near-wake flow of a truck trailer is quite different compared to automotive applications which have been deeply studied. First, the aspect ratio H/W between the height and width of the vehicle is greater than unity. Secondly, the ratio $\lambda = U_s/U_\infty$ between the underflow and the free-stream velocities differ according to the type of vehicle (heavy duty, medium duty, bus, van or square-back car). For example, the λ parameter for a heavy duty can reach down to 0.1 without being higher than 0.3 and for a square-back car, λ is close to unity. Many articles in the literature relate to the ground clearance effect for 2D or 3D models ([1], [2]). For instance, Grandemange et al. [2] have studied the impact of the ground clearance on the near-wake and on the rear base pressure of parallelepiped bodies with a rectangular blunt trailing edge. By changing the ground clearance (contrary to the present study), both the wake interaction with the ground and the underflow velocity are changed. In addition, Perry et al. [3] have studied the impact of the roughness on rear wake structure of a square-back vehicle where an increase in underbody roughness resulted in an increase of the drag. The aim of the present experimental investigation is to study, on a 1:43 scale simplified truck model (Figure 1a), how the underbody velocity modifies the near-wake and the rear base pressure and to understand how the beneficial effect of passive control (boat-tails) depends on underside flow velocities without changing any geometric parameters. Furthermore, this work follows the one of Chaligné [4] for which a combination between pulsed jets and flaps allowed a decrease of the drag. Thus for future studies with pulsed jet system, this study allows to have a detailed knowledge of the reference flow.

The rear part of the model can support two configurations. The first one is a square-back geometry and the second one is a boat-tails geometry with three inclined flaps located on the upper and lateral sides as illustrated in Figure 1b. The experiments are conducted in an open wind tunnel where the free-stream velocity U_∞ is varied from 25 m/s to 40 m/s resulting in a Reynolds number based on the

height H of the model, $1.3 * 10^5 \leq Re_H = U_\infty H/\nu \leq 2.1 * 10^5$. In the present study, flow separation over the upper flap, with a length l/H = 0.12, is avoided thanks to a moderate angle β=15°, in contrast with the case studied by Chaligné [4] on the same geometric model but at a bigger scale. In addition, the model lies on two lateral skirts, guiding the underside flow up to the model rear end. The underbody momentum is adjusted thanks to a pressure loss device (Figure 1c) consisting of grids with various porosity introduced in the ground clearance area. In this study, several pressure losses are investigated within a λ range from 0.08 until 0.84. Even without grid, the λ parameter cannot reach the unity because of the natural pressure loss created by the small cross-sectional underbody area. Static pressure measurements and stereo-PIV in the mid plane are performed to characterize the wake development and its effects on the rear base.

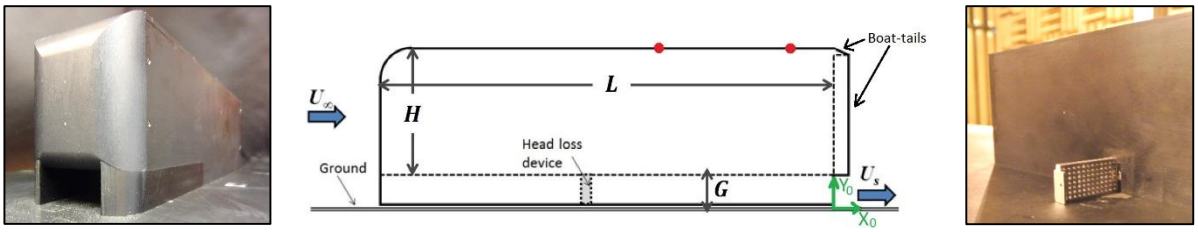

(a) (b) (c)

Figure 1: Nose (a) and side view (b) of the model. The red dots representing the positions of the pressure taps on the roof. Focus on the removable pressure loss system, grids (c). x_0 = 0 corresponds to the plane of the rear base for both configurations.

2. Results and discussion

2.1. The flow around the model

The introduction of pressure losses in the underbody area modifies very slightly the flow just before the nose of the model. Indeed, Figure 2 presents the flow for extremal λ values, one can see that the flow velocity entering in the underbody area is slower for λ = 0.08 (Figure 2a) than for λ = 0.84 (Figure 2b). In addition, the stagnation point is localized higher for λ = 0.84. Nevertheless, for a pressure tap localized in the mid plane in y_0/H=0.81 on the front nose, the pressure coefficient, close to unity, is the same for λ=0.08 to λ = 0.84. Furthermore, for all λ values, the boundary layer thickness growth rate just after the nose of the model is initially high due to a negative axial pressure gradient, but it's not sufficient to cause a flow detachment. In Figure 3 is presented, for all λ values, the pressure coefficient in x_0/H = -0.27 and x_0/H = -1.5 for the two rear configurations and for several Reynolds numbers. First, considering the upper curves (Figure 3a and Figure 3b), the incoming flow at x_0/H = -1.5 is independent of λ since the pressure coefficient stays nearly constant. On the other hand, wall static pressure at the end of the roof (at x_0/H = -0.27, lower curves in Figure 3a and Figure 3b) exhibits a strong influence of λ parameter and also at the rear base configuration. Indeed, the pressure coefficient in boat-tails configuration is twice as small as that of the square-back configuration. In fact, it's a sign that the flow is attached to the boat-tail. For instance, in [4], when the flow is separated to the upper flap, the pressure coefficient is close to -0.2 but when it's attached the pressure coefficient is twice smaller, as in Figure 3c.

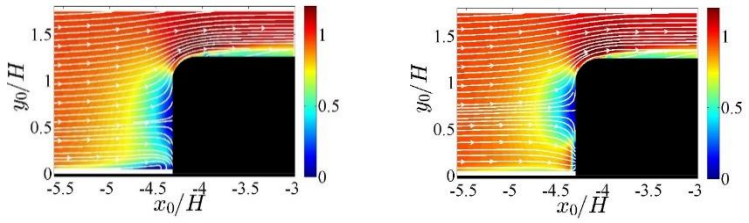

(a) (b)

Figure 2: Non-dimensional velocity of the mid-width plane for λ=0.08 (a) and λ=0.84 (b) in the boat-tails configuration for U_∞ = 25 m/s.

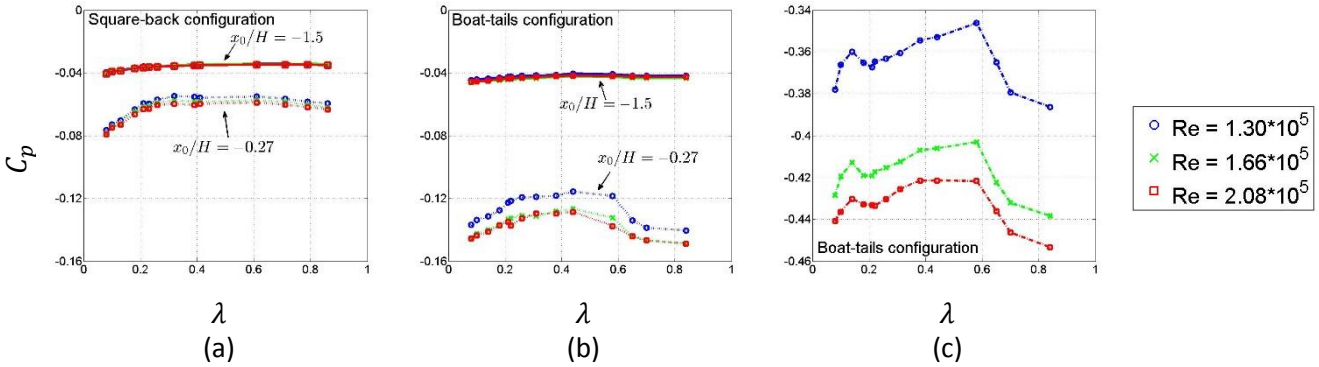

(a) (b) (c)

Figure 3: Pressure coefficient evolution according to λ for several Reynolds numbers. In (a) and (b) are presented the pressure coefficient on the roof and in (c), the pressure coefficients on the upper flap.

2.2. Base pressure and near-wake

The evolution of the mean rear base pressure coefficient C_p with λ is given in Figure 4(a) for both configurations, square-back and boat-tails. For all λ values, the pressure coefficient with the boat-tails configuration is always higher than the square-back configuration (the rear pressure gain is between 30% and 43%). Additionally, the modification in C_p due to variation in λ are small compared to these induced by the boat-tails. Furthermore, the trends in C_p evolution with λ differ substantially from one configuration to the other. For instance, for $\lambda \in [0.23: 0.4]$, C_p barely increase with λ for the boat-tails configuration but largely decrease for the square-back configuration. This highlights the interest of studying the effects of λ on C_p for different rear configuration. These results are consistent with others studies ([5], [6], [7]) where adding flaps improves the drag but for one defined underbody velocity. Nevertheless, it's clear that the underbody velocity, for a fixed rear configuration, modifies the base pressure of the model, until 25% in the both rear configuration. Figure 4b and Figure 4c present the evolution of the vertical and horizontal pressure gradients defined by (1). Whatever the rear configuration the horizontal pressure gradient is nearly null so the pressure distribution is symmetric in the vertical mid plane as for real road vehicles ([8], [9]). The vertical pressure gradient is mostly positive and seems to have the same evolution as the pressure coefficient according to λ. Nevertheless, only in the boat-tails configuration, for $\lambda \geq 0.79$, there are sharp changes in the rear base pressure distribution (the vertical pressure gradient becomes negative) and in the near-wake development. The lower recirculation structure is closer to the base than the upper one for the case λ = 0.58 and conversely for the case λ = 0.86 (see Figure 5 c, d). In addition, an up to down bi-stability phenomenon is observed for λ = 0.65.

$$\frac{\partial C_p}{\partial y^*} = \frac{C_p(up) - C_p(down)}{\Delta y_0/\mathrm{H}} \qquad \frac{\partial C_p}{\partial z^*} = \frac{C_p(left) - C_p(right)}{\Delta z_0/\mathrm{H}} \qquad (1)$$

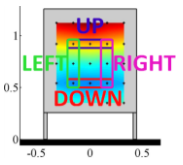

All of these pressure changes are linked to a modification of the near-wake structure. Figure 5 presents the evolution of the wake according to some of λ values for the boat-tails configuration. For λ = 0.08, the wake is similar to one of a backward facing step flow with only one recirculation bubble attached to the ground. Then for λ = 0.32, a recirculation bubble is always attached to the rear base and a second recirculation bubble is now localized on the bottom of the wake. For $\lambda \geq 0.86$, two counter-rotating bubbles detached from the ground formed the wake. In addition, whatever the λ

values, the boat-tails may create longitudinal vortices. We have seen that a change of λ ensues different wake topologies, nevertheless the boat-tails always reduce the drag. One may then ask whether the physical mechanisms responsible for the drag reduction like the evolution of the recirculation area length and height, the shear layer thickness growth rate, the damping of velocity fluctuations in the upper shear layers, the dissipation of turbulent kinetic energy are always the same according to λ.

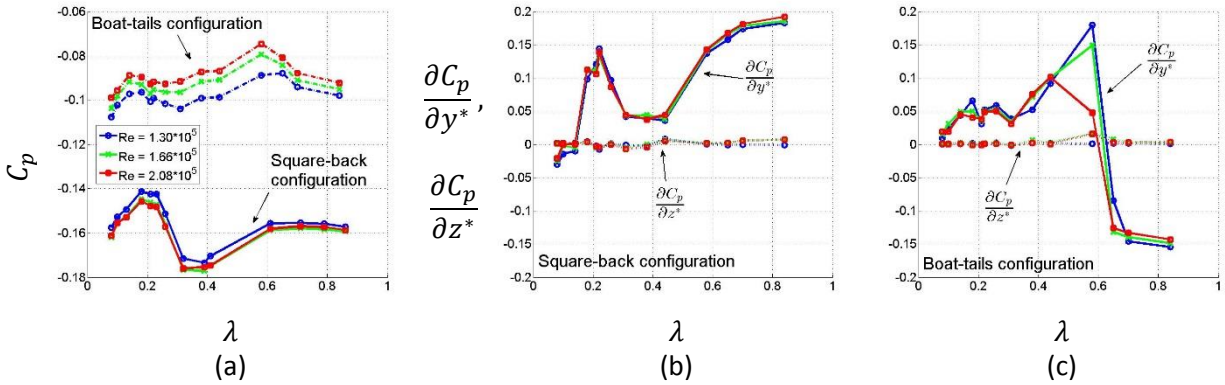

Figure 4: Rear base pressure coefficient C_p(a) evolution according to λ for several Reynolds. Vertical and horizontal pressure gradient evolution according to λ for square-back configuration (b) and boat-tails configuration (c).

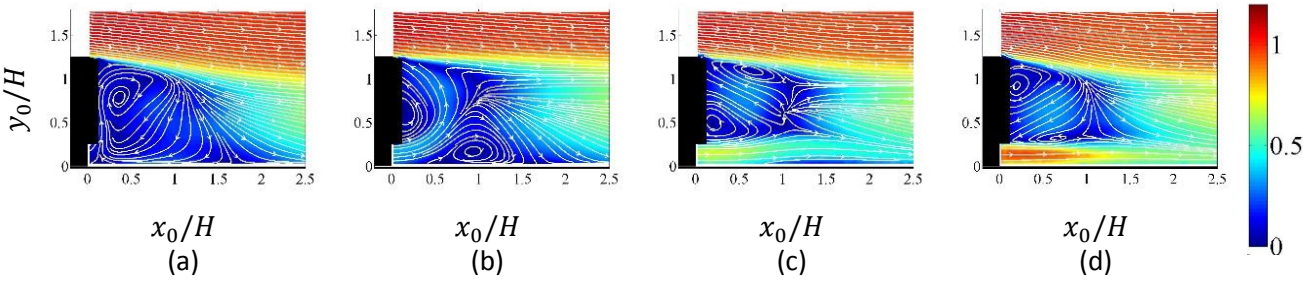

Figure 5: Non-dimensional velocity of the mid-width plane for λ=0.08 (a), λ=0.32 (b), λ=0.58 (c) and λ=0.86 (d) in the boat-tails configuration.

References

[1] K. P. Garry, «Some effects of ground clearance and ground plane boundary layer thickness on the mean base pressure of a bluff vehicle type body,» *Journal of Wing Engineering and Industrial Aerodynamics, 62,* pp. 1-10, 1996.

[2] M. Grandemange, M. Gohlke et O. Cadot, «Bi-stability in the turbulent wake past parallelepiped bodies with various aspect ratios and wall effects,» *Physics of Fluids,* vol. 25, 2013.

[3] A. K. Perry et M. Passmore, «The impact of underbody roughness on rear wake structure of a squareback Vehicle,» *SAE International, 2013-01-0463,* 2013.

[4] S. Chaligné, «Contrôle du sillage d'un corps non profilé - Application expérimentale à une maquette simplifiée de véhicule industriel,» *Thèse de doctorat de l'Université de Lyon,* 2013.

[5] F. Browand, C. Radocich et M. Boivin, «Fuel savings by means of flaps attached to the base of a trailer : field test results,» *SAE paper, 2005-01-1016,* 2005.

[6] D. Landman, R. Wood, W. Seay et J. Bledsoe, «Understanding practical limits to heavy truck drag reduction,» *SAE paper, 2009-01-2890.*

[7] J. Leuschen et K. R. Cooper, «Full-scale wind tunnel tests of production and prototype, second generation aerodynamic drag reducing devices for tractor-trailers,» *SAE paper, 2006-01-3456,* 2006.

[8] O. Cadot, A. Courbois, D. Ricot, T. Ruiz, F. Harambat et e. al., «Characterizations of force and pressure fluctuations on real vehicles,» *International Journal of Engineering Systems Modelling and Simulation, Inderscience,* vol. 8 (2), pp. 99-105, 2016.

[9] M. Grandemange, D. Ricot, C. Vartanian, T. Ruiz et O. Cadot, «Characterization of the flow past real road vehicles with blunt afterbodies,» *International Journal of Aerodynamics, Inderscience,* vol. 24 (1/2), pp. 24-42, 2014.